Reflectivity and polarization dependence of polysilicon single-film broadband photonic crystal micro-mirrors

Sora Kim,[1,*] Sanja Hadzialic,[2] Aasmund S. Sudbo,[3] and Olav Solgaard[4]

[1]*General Electric Global Research Center, 1 Research Circle, Niskayuna, New York 12309, USA*
[2]*SINTEF ICT, Microsystems and Nanotechnology, P.O.Box 124, Blindern, N-0314 Oslo, Norway*
[3]*Department of Physics, University of Oslo, University Graduate Center, P.O. Box 70, N-2027 Kjeller, Norway*
[4]*Department of Electrical Engineering, Stanford University, Stanford, California 94305, USA*
[*]*kims@ge.com*

Abstract: We report on the fabrication of 2-D photonic crystal (PC) micro-mirrors, and Finite Difference Time Domain (FDTD) simulations and measurements of their reflectance spectra and polarization dependence at normal incidence. The PC mirrors were fabricated in free-standing thin polysilicon membranes supported by silicon nitride films for stress compensation. Greater than 90% reflectivity is measured over a wavelength range of 35 nm from 1565 nm to 1600 nm with small polarization dependence. Our FDTD simulations show that fabrication errors on the order of tens of nanometers can strongly affect the reflection spectra. When the fabrication errors are kept below this level, FDTD simulations on perfectly periodic structures accurately predict the reflection spectra of the fabricated PC mirrors, despite their sensitivity to the fabrication errors.

©2011 Optical Society of America

OCIS codes: (230.5298) Photonic crystals; (050.6624) Subwavelength structures; (310.6628) Subwavelength structures, nanostructures; (310.6860) Thin films, optical properties.

References and links

1. L. Mashev and E. Popov, "Zero order anomaly of dielectric coated gratings," Opt. Commun. **55**(6), 377–380 (1985).
2. Z. S. Liu, S. Tibuleac, D. Shin, P. P. Young, and R. Magnusson, "High-efficiency guided-mode resonance filter," Opt. Lett. **23**(19), 1556–1558 (1998).
3. M. C. Y. Huang, Y. Zhou, and C. J. Chang-Hasnain, "A surface-emitting laser incorporating a high-index-contrast subwavelength grating," Nat. Photonics **1**(2), 119–122 (2007).
4. J. Jiang and G. P. Nordin, "Optimal design of sub-wavelength dielectric gratings as broadband mirrors," OFC/NFEC '05, Anaheim, USA (2005).
5. S. Peng and G. M. Morris, "Experimental demonstration of resonant anomalies in diffraction from two-dimensional gratings," Opt. Lett. **21**(8), 549–551 (1996).
6. W. Suh, M. F. Yanik, O. Solgaard, and S.-H. Fan, "Displacement-Sensitive Photonic Crystal Structures Based on Guided Resonance in Photonic Crystal Slabs," Appl. Phys. Lett. **82**(13), 1999–2001 (2003).
7. O. Kilic, M. Digonnet, G. Kino, and O. Solgaard, "Controlling uncoupled resonances in photonic crystals through breaking the mirror symmetry," Opt. Express **16**(17), 13090–13103 (2008).
8. I. W. Jung, S. Kim, and O. Solgaard, "High-reflectivity broadband photonic crystal mirror MEMS scanner with low dependence on incident angle and polarization," J. Microelectromech. Syst. **18**(4), 924–932 (2009).
9. V. Lousse, W. Suh, O. Kilic, S. Kim, O. Solgaard, and S. Fan, "Angular and polarization properties of a photonic crystal slab mirror," Opt. Express **12**(8), 1575–1582 (2004).
10. A. Torkkeli, O. Rusanen, J. Saarilahti, H. Seppa, H. Sipola, and J. Hietanen, "Capacitive microphone with low-stress polysilicon membrane and high-stress polysilicon backplate," Sens. Actuators A Phys. **85**(1–3), 116–123 (2000).
11. J. Yang, H. Kahn, A.-Q. He, S. M. Phillips, and A. H. Heuer, "A new technique for producing large-area as-deposited zero-stress LPCVD polysilicon films: the multipoly process," J. Microelectromech. Syst. **9**(4), 485–494 (2000).
12. S. Boutami, B. Ben Bakir, J.-L. Leclercq, X. Letartre, P. Rojo-Romeo, M. Garrigues, P. Viktorovitch, I. Sagnes, L. Legratiet, and M. Strassner, "Highly selective and compact tunable MOEMS photonic crystal Fabry-Perot filter," Opt. Express **14**(8), 3129–3137 (2006).
13. J. H. Ho, C. L. Lee, T. F. Lei, and T. S. Chao, "Ellipsometry measurement of the complex refractive index and thickness of polysilicon thin films," J. Opt. Soc. Am. A **7**(2), 196–205 (1990).

#153708 - $15.00 USD Received 20 Sep 2011; revised 21 Nov 2011; accepted 24 Nov 2011; published 5 Mar 2012

14. J. A. Monsoriu, E. Silvestre, A. Ferrando, P. Andres, and M. V. Andres, "Sloped-wall thin-film photonic crystal waveguides," IEEE Photon. Technol. Lett. **17**(2), 354–356, 354–356 (2005).
15. J. Topolancik, F. Vollmer, R. Ilic, and M. Crescimanno, "Out-of-plane scattering from vertically asymmetric photonic crystal slab waveguides with in-plane disorder," Opt. Express **17**(15), 12470–12480 (2009).
16. K. Hennessy, A. Badolato, A. Tamboli, P. M. Petroff, E. Hu, M. Atature, J. Dreiser, and A. Imamoglu, "Tuning photonic crystal nanocavity modes by wet chemical digital etching," Appl. Phys. Lett. **87**(2), 021108 (2005).
17. B.-S. Song, T. Nagashima, T. Asano, and S. Noda, "Resonant-wavelength control of nanocavities by nanometer-scaled adjustment of two-dimensional photonic crystal slab structures," IEEE Photon. Technol. Lett. **20**(7), 532–534 (2008).
18. D. M. Beggs, L. O'Faolain, and T. F. Krauss, "Accurate determination of the functional hole size in photonic crystal slabs using optical methods," Photonics Nanostruct. Fundamentals Appl. **6**(3–4), 213–218 (2008).
19. E. Graugnard, D. P. Gaillot, S. N. Dunham, C. W. Neff, T. Yamashita, and C. J. Summers, "Photonic band tuning in two-dimensional photonic crystal slab waveguides by atomic layer deposition," Appl. Phys. Lett. **89**(18), 181108 (2006).
20. S. Fan and J. D. Joannopoloulos, "Analysis of guided resonance in photonic crystal slabs," Phys. Rev. B **65**(23), 235112 (2002).

1. Introduction

Photonic crystal (PC) mirrors are very attractive components because they can achieve reflectivity comparable to that of distributed Bragg reflector (DBR) mirrors in a single dielectric membrane, greatly simplifying integration into optical MEMS and enabling more compact and faster devices. DBR mirrors consist of multiple layers of two dielectric films to achieve almost 100% reflectivity, which is essential to VCSEL.

The history of highly reflective dielectric PC mirrors dates back to sub-wavelength 1-D gratings with one or more dielectric layers [1,2]. Among various dielectric materials used for sub-wavelength 1-D gratings, polysilicon is particularly interesting for telecommunication applications due to its low absorption loss at 1550 nm. Moreover, we can benefit from the current thin film deposition technologies, which can control the thickness of polysilicon films to within a few nanometers.

There have been reports on design and fabrication of polysilicon mirrors based on sub-wavelength 1-D gratings [3,4]. Due to their one-dimensional periodicity, the reflectivities of these mirrors are strongly dependent on the polarization and the incidence angle of the input beam, disqualifying them for use in many miniaturized systems. In contrast to 1-D grating mirrors, 2-D PC mirrors [5–7] with a square lattice of circular holes have no polarization dependence for normal incidence. Moreover, when properly designed, they have small dependence on the incidence angle of the input beam [8,9].

In this paper, we report on a 2-D PC mirror fabricated in a free-standing thin polysilicon membrane with support from a nitride film. These free-standing PC mirrors are useful for applications such as tunable filters and displacement sensors where the optical spectral changes result from the movement of the PCs. However, the stress on thin membranes usually causes significant membrane deformation, degrading optical performances of devices. Typical polysilicon deposition process by low-pressure chemical vapor deposition (LPCVD) generally produces films with high residual stress, causing membrane bending or buckling [10,11]. There are several ways to acquire low stress polysilicon membranes; using a sandwich structure with combined tensile and compressive stress layers, forming corrugations in the diaphragm, or controlling deposition process such as deposition or annealing temperature [11]. In this work we use tensile stressed silicon nitride to mitigate the compressive stress of the polysilicon membrane. We deposit a nitride film on top of the polysilicon membrane to compensate for the compressive stress of the polysilicon membrane. Despite the presence of the nitride film, the 2-D PC mirror achieves a reflectivity higher than 90% over a 35 nm bandwidth centered around 1580 nm. This 2-D PC mirror shows low polarization dependence near normal incidence. In this report, we explain details of the fabrication process, the measurement results, and the effects of inevitable fabrication errors on the reflection spectrum of the PC 2-D mirror.

#153708 - $15.00 USD Received 20 Sep 2011; revised 21 Nov 2011; accepted 24 Nov 2011; published 5 Mar 2012
(C) 2012 OSA

2. Design

The design of the broadband polysilicon 2-D PC mirror with a nitride film is depicted in Fig. 1 (a). It consists of a square lattice of circular holes patterned on a 90 nm thick nitride film and a 450 nm thick polysilicon membrane, which was suspended 920 nm above a silicon substrate. The holes have a pitch of 820 nm and a radius of 328 nm. The pitch and the radius of the PC holes and the thickness of the polysilicon membrane were adapted from the previous work [9] to obtain a broad reflection spectrum with high reflectivity around 1550 nm for out-of-plane incidence. Previously, a single free-standing silicon PC membrane with the same geometrical parameters was found by FDTD calculations to theoretically achieve 95% reflectivity over a 65 nm wavelength range from 1500 nm to 1565 nm and a 15° incident angle range regardless of the polarization and the azimuthal angle of the input plane waves [9]. The thickness of the air gap between the PC membrane and the silicon substrate should be as large as possible, to prevent the PC membrane from adhering to the silicon substrate. On the other hand, the air gap should be kept as small as possible to reduce the oxidation time for the layer that forms the air gap later by being released. The thickness of 920 nm for the air gap in the design proposed in this paper was chosen as a compromise. The thickness of the nitride film was determined by a stress measurement; among different thicknesses of a nitride film deposited on the 450 nm thick polysilicon film on top of a thermally oxidized silicon substrate with a 920 nm thick oxide layer, 90 nm was the thickness that best compensated the compressive stress by the polysilicon and oxide layers.

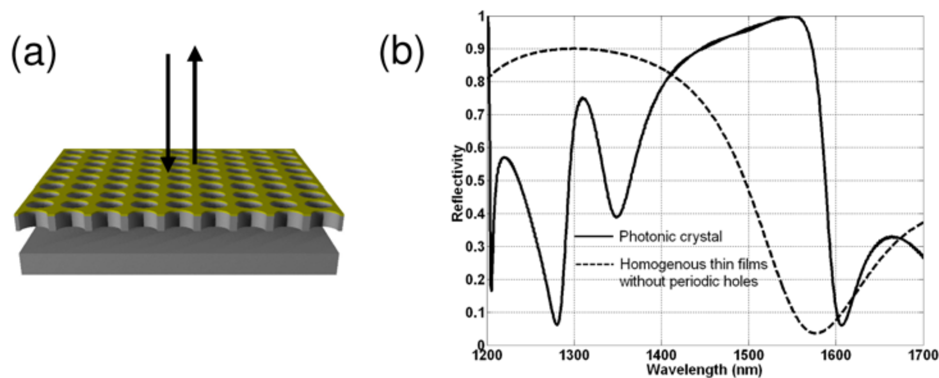

Fig. 1. (a) The broadband polysilicon 2-D PC mirror has a square lattice of circular holes with a pitch of 820 nm and a radius of 328 nm. These holes are patterned on a 90 nm thick nitride film and a 450 nm thick polysilicon membrane, which are suspended 920 nm above a silicon substrate. The nitride film is deposited on top of the polysilicon membrane for stress compensation. In our study, we measure the reflection spectrum of the 2-D PC mirror for normal incidence as indicated in the figure by arrows. (b) FDTD-calculated reflection spectra of the PC mirror (solid) and homogeneous thin films of nitride and polysilicon above a silicon substrate without PC holes (dashed) for normal incidence. Both structures have the same thicknesses of nitride and polysilicon films and an air gap above the silicon substrate. The reflectivity of the PC mirror is higher than 95% from 1490 nm to 1568 nm due to the effect of the periodic PC holes patterned though the thin films on the reflection of the PC mirror.

Although the thicknesses of the air gap and the nitride film were chosen for practical convenience to fabricate PC mirrors on free-standing thin membranes, which could be potentially integrated with MEMS devices, it is important to check if the fabricated PC mirror achieves the desired optical performance with the nitride film and the silicon substrate. As shown in Fig. 1 (b), FDTD calculations show that the PC mirror of the new design could theoretically achieve 100% reflectivity at 1550 nm with reflectivity higher than 95% from 1490 nm to 1568 nm, comparable to the performance of the previous design. This high reflectivity from 1490 nm to 1568 nm is primarily due to the periodic PC holes patterned through the nitride and polysilicon films. For the same wavelength range, the reflectivity is

#153708 - $15.00 USD Received 20 Sep 2011; revised 21 Nov 2011; accepted 24 Nov 2011; published 5 Mar 2012
(C) 2012 OSA

lower than 50% for a mirror without PC holes, consisting of only homogenous thin films of the nitride and polysilicon with the same thicknesses and distance above the silicon substrate.

It is interesting to note that the air-gap and the silicon substrate help maintain the bandwidth despite the additional nitride film. The nitride film alone tends to reduce the reflectivity of the single free-standing polysilicon PC mirror. Compared to the reflection spectrum of the previous design, which is shown as a black solid line in Fig. 2, the reflection spectrum of the PC mirror with the nitride film on top of the free-standing polysilicon membrane shows significant reflectivity drop around 1350 nm as shown in Fig. 2 (black dotted line). Interestingly, the reflectivity at 1550 nm, where the guided resonance achieved 100% reflectivity in the previous design, is still 100% despite the fact that the vertical mirror symmetry of the PC slab is broken. The reflectivity drop can be explained by the fact that the effective refractive index of the PC membrane is reduced due to the lower refractive index of the nitride film than the polysilicon membrane. The black dashed line in Fig. 2 is the reflection spectrum of the PC mirror with a 920nm air-gap and a silicon substrate in addition to the nitride film. The reflectivities at certain wavelengths increase by additional constructive interference between the reflection from the PC layer and the reflection from the silicon substrate, theoretically achieving a bandwidth comparable to that of the previous design.

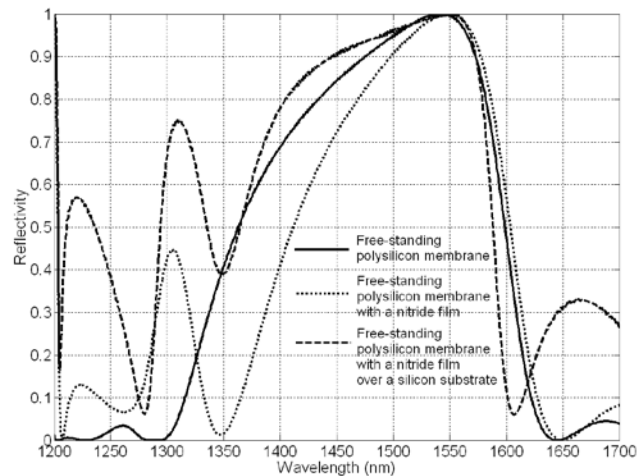

Fig. 2. FDTD-calculated reflection spectra of 2-D PC mirrors, for three different mirror structures. The calculations were done for a free-standing polysilicon membrane, for a membrane with an additional nitride film, and for a composite membrane over a silicon substrate like the structure shown in Fig. 1 (a). The black solid line is a reflection spectrum of a 2-D PC mirror consisting of a square lattice of circular holes with a pitch of 820 nm and a radius of 328 nm. These circular holes are patterned in a free-standing 450 nm thick silicon membrane. This 2-D PC mirror achieves 100% reflectivity at 1550 nm and 95% reflectivity from 1500 nm to 1560 nm. The black dotted line is a reflection spectrum of a 2-D PC mirror of the same structure except for having an additional 90 nm thick nitride film on top of the free-standing silicon membrane. The reflectivity at 1550 nm is still 100%, but the reflectivities at wavelengths lower 1550 nm decreases, reducing the bandwidth of the spectrum with 95% reflectivity. A silicon substrate under the PC membrane with a 920 nm thick air-gap between them increases the bandwidth. (Black dashed line) The reflectivity is higher than 95% at wavelengths from 1490 nm to 1568 nm.

The design proposed in this paper has several fabrication advantages over the previous design [8]. It allows the thickness of the PC layer to be accurately controlled by thin-film deposition. Also, the thin-film deposition can provide more flexibility of integrating thin PC membranes with other devices such as MEMS devices that require more complicated fabrication processes. Furthermore, there is no need to remove the thick silicon substrate, which simplified the fabrication process. Substrate removal usually requires a long and aggressive etch process, resulting in low process yield.

#153708 - $15.00 USD Received 20 Sep 2011; revised 21 Nov 2011; accepted 24 Nov 2011; published 5 Mar 2012
(C) 2012 OSA

3. Fabrication

The fabrication process is described in Fig. 3. A silicon wafer is thermally oxidized to produce a 920 nm thick oxide film. To create the 2-D PC, a 450 nm thick polysilicon film and a 90 nm thick nitride film are deposited on top of the oxide film by low-pressure chemical vapor deposition (LPCVD). The nitride film is deposited to compensate for the compressive stress of the polysilicon film and produce a flat membrane. Then, an 1 µm thick polymethyl methacrylate (PMMA) layer is spun on the wafers, and an area of 100 µm x 100 µm is patterned with PC holes in the PMMA layer by a Hitachi H-700 F11 electron beam lithography machine. After PMMA development, the PC holes on the developed PMMA are transferred to the nitride and the polysilicon films by reactive ion etching in an Applied Materials p5000 etcher. CHF_3 and a combination of Cl_2 and HBr are used to etch the nitride and the polysilicon films, respectively. The PMMA is then stripped off, and finally the PC membrane is released by removing the 920 nm thick thermal oxide layer in 49% liquid HF solution, leaving an air gap between the PC layer and the silicon substrate.

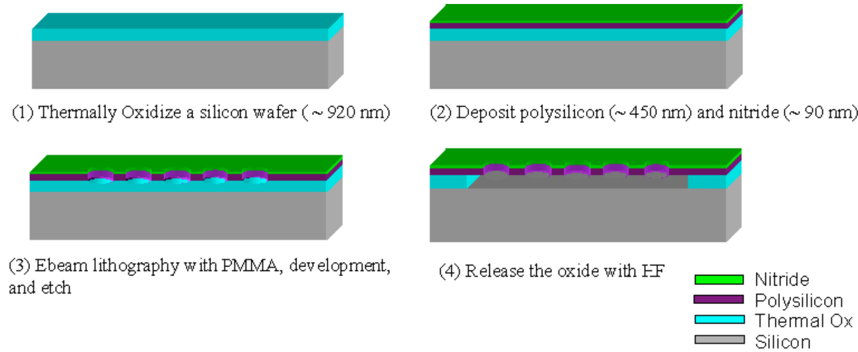

Fig. 3. Fabrication of broadband polysilicon PC mirrors. (1) A silicon wafer is thermally oxidized to define the gap between the PC membrane and the substrate. (2) Polysillicon and nitride layers are deposited on the oxide. These polysilicon and nitride layers compose the PC membrane. (3) PC holes are patterned in the polysilicon and nitride by ebeam lithography and reactive ion etching. (4) The oxide is removed under the PC in liquid Hydrofloric acid (HF), forming a gap between the PC membrane and the substrate.

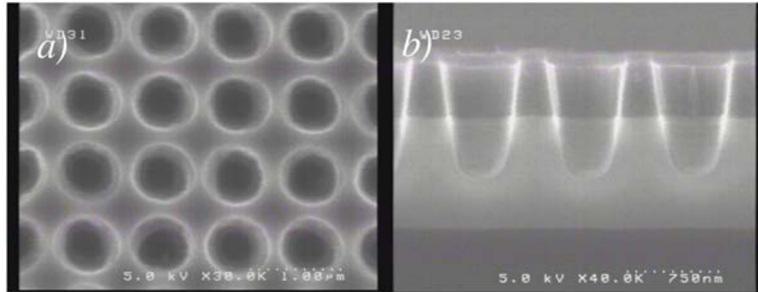

Fig. 4. SEM images of the fabricated broadband PC mirror. These pictures are taken before the oxide layer was removed by hydrofluoric acid etch. (a) Top view: square lattice of holes with 820 nm pitch and 672 nm diameter (b) Side view after wafer cleaving to see the profile of etched holes. From the top: 90nm nitride, 450 nm polysilicon, 920 nm oxide. The etch profiles are from a triangular-lattice PC with the same radius as the square lattice PC. A triangular lattice was chosen for imaging purposes to guarantee that a cleave would reveal the hole cross-section.

The SEM images in Fig. 4 (b) show that the sidewalls of the etched PC holes are not vertical. The boundaries between materials are clearly seen in the figure. Membrane flatness is crucial for optimum mirror performance, but is difficult to achieve in free-standing, miniaturized mirrors designed for optical MEMS. For example, it has been reported that

#153708 - $15.00 USD Received 20 Sep 2011; revised 21 Nov 2011; accepted 24 Nov 2011; published 5 Mar 2012
(C) 2012 OSA

downward bending of a PC membrane significantly degrades the quality factors of tunable Fabry-Perot filters with 1-D InP PC membranes [12]. When released, the polysilicon membrane with the nitride film showed good flatness over a circular region with a radius of 35 µm. The height difference between the center and the edge of the membrane over the circular region was 110 nm, which corresponded to λ/15. If we were to assume that the membrane curvature were uniform, this height difference would correspond to a radius of curvature of the mirror of about 6 mm $\approx (35\mu m)2/(0.22\mu m)$. A spherical mirror like that has a focal length of 3mm, a fairly typical focal length for the lenses used in our measurement setup.

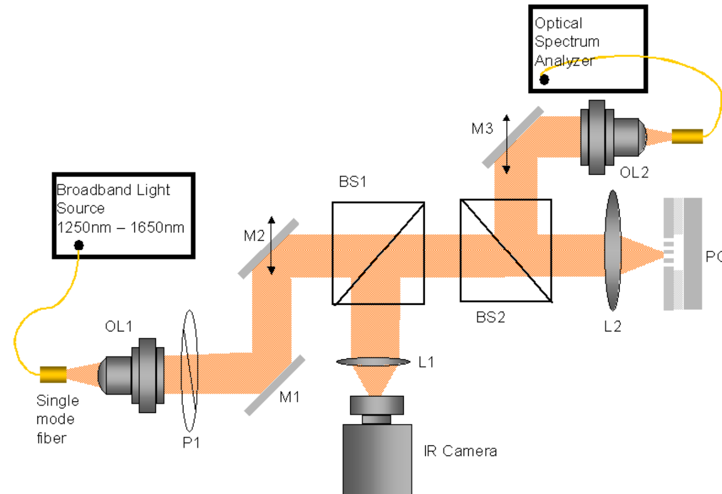

Fig. 5. Schematic of the experimental setup to measure the reflectivity, polarization dependence, and angular dependence of the broadband polysilicon PC mirror. The input beam from an un-polarized broadband super luminescent diode light source is collimated by an objective lens (OL1), sent through a linear polarizer (P1) and beam splitters (BS1 and BS2), and focused onto the PC mirror by a lens L2. The reflected beam from the PC mirror is directed by BS2 and focused onto the single mode fiber connected to the optical spectrum analyzer. The beam splitter, BS1, helps in aligning the PC mirror to the focused beam by allowing an image of the PC mirror and the focused beam to be captured by the IR camera. P1 determines the polarization of the input beam.

4. Measurements and discussion

4.1 Measurement setup and method

Figure 5 shows the measurement setup used to measure reflectivity and polarization dependence of the 2-D PC mirror. We used an un-polarized broadband BWC-SLD super luminescent diode light source with a wavelength range from 1250 nm to 1650 nm, manufactured by B&W Tek, Inc. The light from the source is collimated by an objective lens (OL1), sent through a linear polarizer (P1) and beam splitters (BS1 and BS2), and focused onto the PC mirror. The radius of the focused beam on the PC mirror is smaller than 35 µm, which is the radius of the relatively flat area of the PC mirror. The linear polarizer, P1, determines the polarization of the input beam. The beam splitter, BS1, allows the focused beam on the PC mirror to be imaged with an IR camera, making it convenient to position the beam on the PC mirror. The beam splitter, BS2, directs the reflected beam from the PC mirror, which is collimated by L2, onto OL2, which couples the beam to a single mode fiber connected to an optical spectrum analyzer. A gold-coated mirror of known reflectivity (96% over the wavelength range from 1250 nm to 1650 nm provided by Newport) was used as a reference to calculate the absolute reflectivity of the PC mirror.

4.2 Reflectivity and polarization dependence at normal incidence

The reflectivity for normal incidence was measured for two orthogonal linear polarizations of the input beam. The reflectivity was higher than 90% from 1565 to 1600 nm for both polarizations as shown in Fig. 6 (dashed and dotted lines). The two spectra showed a very similar dependency on wavelength. The small degree of polarization dependence is due to fabrication imperfections.

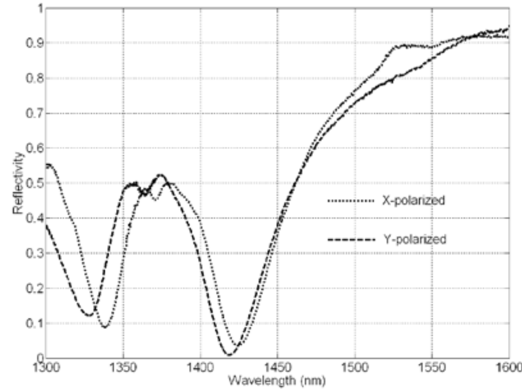

Fig. 6. Measured Reflection spectra for two orthogonal linear polarizations for normal incidence (dashed and dotted lines). The low, but non-zero, polarization dependence of the PC mirror at normal incidence is assumed to be due to fabrication imperfections. The reflectivity is higher than 90% from 1565 nm to 1600 nm.

In Fig. 7 (a), the experimental (dashed and dotted) and theoretical (solid) reflection spectra are superimposed. The differences are presumably caused by structural and optical variations introduced to the PC mirror during the fabrication process, such as a refractive index of polysilicon different from that of silicon, expanded PC holes, and sloped PC sidewalls. When these fabrication variations were incorporated into the PC model of FDTD calculations, the calculated spectrum in Fig. 7 (b) showed very good agreement with the measured spectrum. These results imply that although these variations caused a significant change in the spectrum, the FDTD calculations can predict the spectral change if these variations are included properly in the PC model used for the FDTD calculations. This will be explained further in the next section.

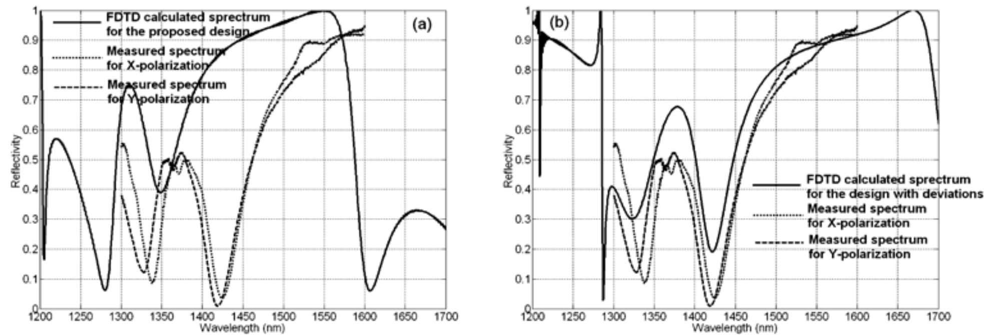

Fig. 7. (a) The comparison between the measured reflection spectra (dashed and dotted lines) and the FDTD calculated (solid line) reflection spectrum for the proposed design. It shows a significant discrepancy between the measurement and the calculation. (b) The FDTD calculation shows very good agreement with the measurement after incorporating the experimentally observed deviations from design in the fabricated device.

#153708 - $15.00 USD Received 20 Sep 2011; revised 21 Nov 2011; accepted 24 Nov 2011; published 5 Mar 2012
(C) 2012 OSA

4.3 Fabrication variations and the effect of the nitride film on reflectivity

Several unintended variations introduced during the fabrication process resulted in PC mirrors with a different structure and a different refractive index than what was assumed in the original design. These changes caused a different reflection spectrum of the PC mirror than the spectrum anticipated from the original design as shown in Fig. 7. We performed FDTD calculations for a new PC model with the fabrication variations included. Although in reality all the variations changed the reflection spectrum of the PC mirror in a combined fashion, we performed the FDTD calculations by adding up the fabrication variations to the PC model step-by-step to show the accuracy required to control the fabrication process.

First, the actual refractive index of the deposited polysilicon was measured to be 3.7, as recorded by a J.A. Woollam M2000 Spectroscopic Ellipsometer. This value is within the range of previously measured refractive indices of polysilicon films with thicknesses of 150 – 600 nm deposited by chemical vapor deposition [13]. The material loss of polysilicon is low around 1550 nm, so the imaginary part of the refractive index could be ignored. The refractive index of 3.7 is significantly higher than the silicon refractive index of 3.48 used for the initial design. This change in refractive index of polysilicon caused a red-shift as seen in Fig. 8 (a). Second, the SEM images of Fig. 4 revealed that the radius of the PC holes increased from 328 nm to 336 nm, shifting the peak-reflectivity wavelength of the reflection spectrum in Fig. 8 (a) from 1620 nm to 1560 nm (Fig. 8 (b)). The radius expansion could result from several factors during the fabrication process such as the dose of electrons during the e-beam lithography, the concentration of the developer and the time of the PMMA development, the etching time and the ratio of the gas etchants used to etch the PC holes. Lastly, the sloped sidewalls of the PC holes led to a marked red shift of the spectrum in Fig. 8 (b) as shown in Fig. 8 (c). To simulate the influence of the slope of sidewalls on reflectivity, we increased the slope of the sidewalls in small steps until we found a spectrum closest to the measured one. It is difficult to empirically measure the exact value of the sidewall slope, because the sidewall slope is sensitive to etching conditions and varies from hole to hole. By simulation, we found that the calculated reflection spectrum became closer to the measured spectrum as the sidewall slope increased. In Fig. 8 (c), where the calculated reflection spectrum shows the best fit to the measured reflection spectrum, the radius of the PC holes in the FDTD simulation was decreased from 336 nm to 295 nm in steps of 4.1 nm, from top to bottom of the PC holes, corresponding to a slope of 10.97, which fits reasonably well with our experimental observation of a slope of 10.2 in the cross-section SEM picture of Fig. 4. The change of the spectrum due to sidewall slope indicates that etching profiles, in addition to hole pitch and radius, must be controlled accurately to obtain the desired spectrum. This observation agrees with the conclusions made by Monsoriu et al. and Topolancik et al. on the effects of PC sloped sidewalls [14,15]. The slopes of PC sidewalls should be included as one of the design parameters due to the significance of spectral changes by sloped sidewalls of PCs.

The final spectrum in Fig. 8 (c) includes all the deviations from the initial design: the different refractive index of the polysilicon, the larger openings of the PC holes, and the sloped sidewalls of the PC holes. The initially intended reflection spectrum significantly changed due to the fabrication deviations. Different research groups also have discussed the high sensitivity of optical performances of photonic crystals to the variations of geometrical dimensions such as the hole diameter [16–18] or the thickness [19] of photonic crystals. Due to the high sensitivity of photonic crystals, they controlled the hole diameter or the thickness of the photonic crystals by steps smaller than 10 nm to tune the optical spectra of their photonic crystals. The FDTD calculations done in our study also show that the similar level of process control accuracy is required.

Although the spectrum of the photonic crystal mirror is very sensitive to the fabrication variations, the final spectrum in Fig. 8 (c) shows excellent agreement with the measured spectrum. FDTD calculations can accurately predict the spectrum by properly including these deviations in the model for the FDTD calculations.

#153708 - $15.00 USD Received 20 Sep 2011; revised 21 Nov 2011; accepted 24 Nov 2011; published 5 Mar 2012
(C) 2012 OSA

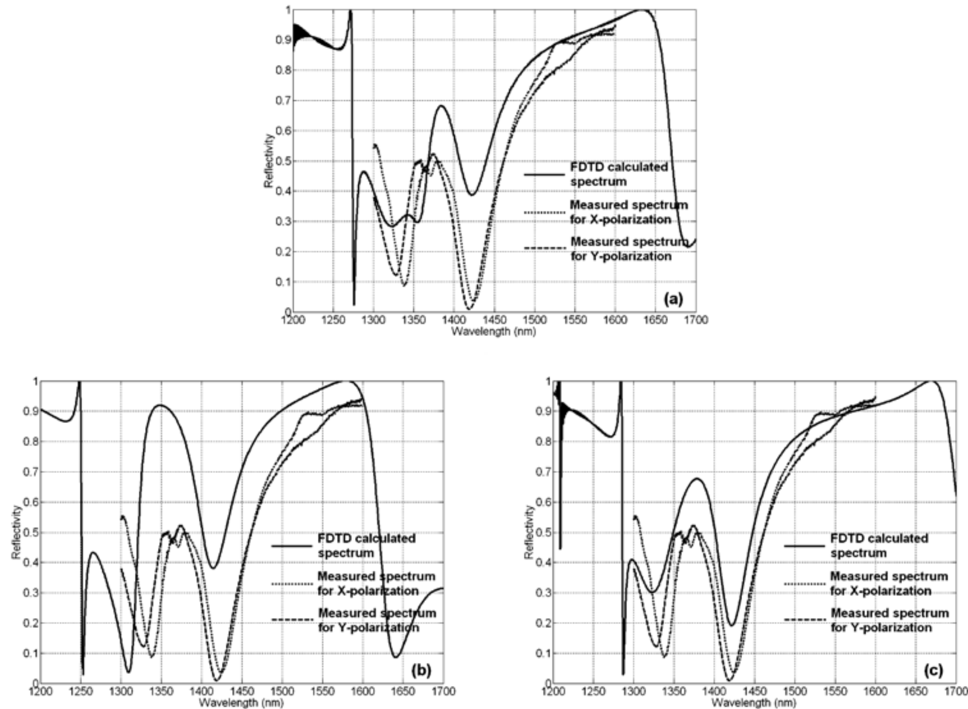

Fig. 8. FDTD calculations of spectral reflectivity as a function of fabrication variations. Each fabrication variation is added to the PC model at each FDTD calculation. (a) The PC model is the same as the one used for the FDTD calculation in Fig. 1 (b) except the refractive index of the polysilicon layer. The actual polysilicon refractive index was 3.7, causing a red-shift of the reflection spectrum calculated for the original design as shown in Fig. 7 (a). (b) The increased radius of the PC holes was added to the PC model. The radius of the PC holes increased by 8nm after PMMA development and RIE etch, causing a blue-shift. (c) The sloped sidewalls of the PC holes were added to the PC model. The sloped sidewalls of the PC holes shifted the high reflectivity region to longer wavelengths. In the FDTD simulations, the PC model has a radius that is decreased step-wise from 336 nm to 295 nm in steps of 4.1 nm over the 450 nm thickness of the PC holes.

In the previous design, the guided resonance of the PC mirror, which is induced by the periodic refractive index modulation, contributes to the 100% reflectivity at 1550nm. As seen in Fig. 8 (c), all the fabrication variations shifted the wavelength with 100% reflectivity to the higher wavelength region. However, the measured reflectivity higher than 90% at 1550 nm was still due to the refractive index modulation. Although the guided resonance peak was shifted to the wavelength region higher than 1600 nm, the reflectivity enhancement occurred at a wide wavelength range because the guided resonance peak is broad due to the big PC holes [20].

The influence of the sloped sidewalls on the reflection spectrum is very interesting. Obviously, the sloped sidewalls of PC holes changed in the spectrum, causing a redshift of the resonance peak. In addition to the nitride film on top of the polysilicon membrane, the sloped sidewalls of PC holes break the vertical mirror symmetry of the guided resonance modes. Previously separated TE-like and TM-like modes are now mixed and interact with each other [14]. Due to this mode mixing, the band gap of PCs gets wider. Moreover, the curvature of the dispersion curves at the band edge is also reduced by the sloped sidewalls [14]. To understand changes in guided resonance modes, it is important to understand the changes that occur at the band edges, because the frequencies of the guided resonance mode are determined by the mode frequencies at the band edges. The wider band gap edge causes the shift of the resonance peak in the wavelength region. The flatter band at the edge contributes to the

#153708 - $15.00 USD Received 20 Sep 2011; revised 21 Nov 2011; accepted 24 Nov 2011; published 5 Mar 2012
(C) 2012 OSA

greater Q factors of the guided resonances, which also explains the sharper resonance peak shown in the FDTD calculations.

5. Conclusion

We have designed and fabricated a 2-D photonic crystal (PC) micro-mirror, and report on measurements and numerical simulations of the spectrum and the polarization dependence of the reflectance of the mirror. The 2-D PC mirror was fabricated on a polysilicon membrane with a nitride film to compensate for compressive stress, and we achieved high reflectivity and small polarization dependence. The measurements show a reflectivity greater than 90% from 1565 nm to 1600 nm and small polarization dependence for two perpendicular linear polarizations of the input light. The simulations show a wavelength range of nearly 100nm around 1550 nm with greater than 95% reflectivity and no polarization dependence of the reflectivity at normal incidence due to the PC's four-fold rotational symmetry.

Initially, we were unable to get agreement between the simulations and measurements of spectral reflectivity. SEM images of the fabricated devices revealed, however, deviations in the device geometry from the intended design. Our FDTD calculations show that any small unintended deviations from the initial designs of PC mirrors can dramatically change their spectra. We demonstrate that the measured reflectance spectrum could be very closely replicated from the calculated reflectance spectrum by adding the experimentally observed deviations to the PC model for the FDTD calculations. This implies that once the sources of the deviations are known, the spectral changes can be accurately anticipated by FDTD calculations. Our calculation results show that for FDTD-calculated spectra to agree with measurements, the PC-mirror geometry has to be very accurately represented. One of the most sensitive parameters is the diameter of the holes of the PC, which should be accurate to better than at least 8nm.

Polysilicon thin-film technology provides flexibility in design and fabrication of PC mirrors integrated with optical MEMS without sacrificing optical functionality. However, control of the fabrication process, structural definition, and internal stress of the deposited films are still hurdles in obtaining desirable performances. The optical spectra of photonic crystals are very sensitive to geometrical variations caused by fabrication errors. However, this high sensitivity may also lead to useful PC sensors.

#153708 - $15.00 USD Received 20 Sep 2011; revised 21 Nov 2011; accepted 24 Nov 2011; published 5 Mar 2012
(C) 2012 OSA